

SCIENTIFIC REPORTS

OPEN

Inactivation of HMGCL promotes proliferation and metastasis of nasopharyngeal carcinoma by suppressing oxidative stress

Wenqi Luo¹, Liting Qin¹, Bo Li², Zhipeng Liao³, Jiezhen Liang³, Xiling Xiao³, Xue Xiao³, Yingxi Mo⁴, Guangwu Huang³, Zhe Zhang³, Xiaoying Zhou⁵ & Ping Li¹

Altered metabolism is considered as a hallmark of cancer. Here we investigated expression of 3-hydroxy-3-methylglutaryl-coenzyme A (HMG-CoA) 2 lyase (HMGCL), an essential enzyme in ketogenesis, which produces ketone bodies by the breakdown of fatty acids to supply energy, in nasopharyngeal carcinoma (NPC). The expression of HMGCL was silenced in NPC tissue. Downregulation of HMGCL in NPC was associated with low intracellular β -hydroxybutyrate (β -HB) production, thereby reducing reactive oxygen species (ROS) generation. Ectopic expression of HMGCL restored β -HB level, associated with suppressed proliferation and colony formation of NPC cells *in vitro* and decreased tumorigenicity *in vivo*. HMGCL suppressed the migration and invasion of NPC cells *in vitro* via mesenchymal-epithelial transition. Furthermore, extracellular β -HB supply suppressed the proliferation and migration of NPC cells. Both intra- and extracellular β -HB exerting a suppressive role in NPC depends on ROS generation. Ketogenesis may be impaired in NPC cells due to lack of HMGCL expression, suggesting that it may be a promising target in NPC therapy.

Nasopharyngeal carcinoma (NPC) is a malignancy frequently originating in the slit-like nasopharyngeal recess called fossa of Rosenmüller. NPC is associated with distinct geographical, racial and ethnic distribution¹. The incidence of NPC is less than 1/100,000 people worldwide, but the cancer is endemic in Southeast Asia and southern China, with an incidence of 20 to 30/100,000 people². Multiple factors are involved in the carcinogenesis of NPC, including genetic susceptibility, environmental factors and Epstein-Barr virus (EBV) infection^{1,2}. NPC is conventionally treated with radiotherapy and early-stage NPC can be cured this way, but a significant number of patients still show local recurrence and distant metastases, so novel strategies for NPC therapy are needed³.

The development and progression of malignancy is accompanied by altered metabolism of tumor cells, considered as a hallmark of cancer⁴. This metabolic reprogramming of tumor cells facilitates their adaption to the tumor microenvironment, which provides the needed energy to sustain their malignant behavior, including accelerated proliferation, apoptosis resistance, evasion of immune attack, and maintenance of a cancer stem cell state⁵⁻⁷. One of the well-known strategies used by tumor cells is the Warburg effect, whereby tumor cells “ferment” glucose to lactate via aerobic glycolysis to generate ATP despite abundant oxygen⁸. The metabolic switch of NPC could be regulated by EBV-encoded products^{9,10}, cellular genes¹¹, long non-coding RNAs (LnRNAs)¹², and microRNAs¹³, targeting the glucose transporters and glycolytic enzymes.

The intermediate product of glycolysis, acetyl-CoA, is a main ingredient for fatty acid (FA) synthesis. Intracellular long-chain FAs are metabolized to be stored as neutral lipids. FAs are esterified to produce triglycerides and phospholipids or used for energy production and transfer, then FAs are oxidated. The oxidative metabolism of FAs yields CO₂ as its end product or FAs are incompletely metabolized to ketone bodies, which can be

¹Department of Pathology, First Affiliated Hospital of Guangxi Medical University, Nanning, China. ²Department of Radiotherapy, First Affiliated Hospital of Guangxi Medical University, Nanning, China. ³Department of Otolaryngology-Head & Neck Surgery, First Affiliated Hospital of Guangxi Medical University, Nanning, China. ⁴Department of Research, Affiliated Tumor Hospital of Guangxi Medical University, Nanning, China. ⁵Life Science Institute, Guangxi Medical University, Nanning, China. Wenqi Luo and Liting Qin contributed equally to this work. Correspondence and requests for materials should be addressed to X.Z. (email: zhouxiaoying1982@foxmail.com) or P.L. (email: liping@gxmu.edu.cn)

secreted and used by neighbor cells^{14,15}. Fast-proliferating tumor cells have a high requirement for lipids (FAs and cholesterol), which are used mainly for biosynthesis of structural components of the cellular membrane, as well as for production of energy during nutrient deprivation¹⁶.

Various kinds of tumors increase their capacity to synthesize FAs and store them as lipid droplets (LDs)^{17–19}. The accumulation of LDs is associated with the expression of other “stemness” markers in colorectal and glioma cancer stem cells^{18,20}. We observed that LDs accumulate in human NPC cell lines and primary tumor tissues^{21,22}. EBV infection can modulate FA synthesis by upregulating the expression of FA synthase and lipogenesis²³. Preclinical and clinical studies have demonstrated an anticancer effect of drugs interfering with FA β -oxidation or lipid synthesis²⁴. However, the molecular mechanisms involved in altered lipid metabolism in NPC remain unclear.

Another metabolic conversion of FA is ketogenesis. Ketone bodies, that is, β -hydroxybutyrate (β -HB), acetoacetate (AcAc), and acetone, are mainly produced in the liver. Besides occurring in hepatocytes, ketone body production and release has been shown in normal epithelial cells and tumors^{25–27}. The ketogenesis and function of ketone bodies in tumorigenesis and tumor progression has been under debate. Certain kinds of tumor cells use ketone bodies in proliferation and metastasis²⁸ (e.g., increasing the intracellular level of acetoacetate specifically promotes activation of MEK-ERK signaling in melanoma²⁷). However, in some malignancies such as brain and gastric cancers, tumor cells cannot effectively use ketone bodies for energy. Extracellular ketone bodies have strong anti-proliferative and pro-apoptotic effects in several cancers, including pancreatic and gastric cancer, as well as EBV-positive lymphoblasts^{29–31}. In addition, ketone bodies affect intracellular oxidative stress³², which is crucial for the survival and function of tumor cells³³.

3-Hydroxy-3-methylglutaryl-coenzyme A (HMG-CoA) 2 lyase (HMGCL) catalyzes the cleavage of HMG-CoA into acetyl-CoA and acetoacetate to mediate the rate-limiting step in the metabolic processing of ketone bodies for energy production³⁴. To date, only a few studies have verified the role of HMGCL in human cancers. HMGCL was found upregulated in androgen-independent prostate cancer cells and BRAF-mutated melanoma^{26,27}. In breast cancer, HMGCL and other enzymes associated with ketone-body production were preferentially expressed in the tumor stroma³⁵. The oncogenic Kaposi’s sarcoma-associated herpesvirus was shown to interfere with transcription of HMGCL directly by targeting its promoter region³⁶.

Here, we investigated the expression and possible role of HMGCL in NPC. Because HMGCL is a key enzyme in ketogenesis, we analyzed the effect of both intracellular and extracellular ketone-body production on the malignant behavior of NPC cells and examined the possible mechanisms involved.

Results

Identification of differentially expressed ketogenesis genes in NPC tumors. To understand the reprogramming of genes participating in regulating lipid metabolism in NPC, we used microarray data from the GEO database (GSE 12452), including 30 cases of NPC tissue and 9 cases of normal nasopharyngeal epithelium (NNE). We found 41 genes with differential expression between the 2 tissue types. Two genes, *HMGCL* and *BDH1*, both involved in the ketogenesis pathway, were significantly downregulated in NPC tissue (Fig. 1a), which suggests altered ketone-body metabolism. We further analyzed microarray data from the GSE 53819 database including 18 cases of NPC and 18 cases of NNE controls. In this screen, we found 2 genes involved in ketogenesis, *HMGCL* and *ACAT1* (data not shown). The *HMGCL* gene was selected for further study.

The expression of HMGCL is downregulated in NPC. To confirm our microarray data, we firstly investigated the transcriptional level of *HMGCL* in NPC samples by quantitative real-time PCR. As compared with an immortalized normal nasopharyngeal epithelial cell line (NP69), 6 NPC cell lines (CNE1, CNE2, HONE1, HK1, 5-8 F and 6-10 B) showed reduced mRNA level of *HMGCL* (Fig. 1b). As well, the expression of the *HMGCL* gene was downregulated in 23 NPC primary tumors but easily detected in all 21 NNE samples (Fig. 1c). In summary, in all 23 NPC cases tested, the expression of *HMGCL* was significantly lower than the mean *HMGCL* expression in NNE samples ($p < 0.05$, Fig. 1c).

In addition, we measured the protein levels of HMGCL in NPC tissue by immunohistochemical (IHC) staining. HMGCL was localized in the cytoplasm of cells and was highly expressed in the NNE layer ($n = 21$) (Fig. 2) but was almost absent in NPC tissue ($n = 30$). This finding further supports our finding that *HMGCL* is transcriptionally inactivated in NPC.

HMGCL increases intracellular level of β -hydroxybutyrate (β -HB) and acetoacetate (AcAc) and generates ROS in NPC cells. To understand the possible function of HMGCL, we stably transfected NPC cells with an HMGCL construct or the corresponding empty-vector pCMV6-Entry construct. We assessed the relative concentration of intracellular β -HB and AcAc, the main components of ketone bodies in HMGCL-HK1 and pCMV6-Entry-HK1 cells. Both intracellular β -HB and AcAc level was significantly higher with HMGCL-HK1 than pCMV6-Entry-HK1 (Fig. 3a), which suggests that HMGCL expression directly contributes to ketogenesis in NPC cells.

Because ketone bodies could increase ROS production³⁷, we further analyzed the association between intracellular/extracellular β -HB and ROS level. β -HB generated by ectopic expression of HMGCL as well as extracellular β -HB treatment elevated ROS production in NPC cells (Fig. 3b,c), so the effect of HMGCL expression in NPC cells may be mediated by ROS.

Exogenous expression of HMGCL suppresses NPC cell proliferation *in vitro* and *in vivo*. To explore the functional role of *HMGCL* in cell growth, we compared the proliferation of *HMGCL*-HK1 and *HMGCL*-5-8F cells to corresponding control cell lines pCMV6-Entry-HK1 and pCMV6-Entry-5-8F by MTT assay. HMGCL was expressed in *HMGCL*-HK1 and *HMGCL*-5-8F cells (Fig. 4a). HK1/5-8F cells transfected with

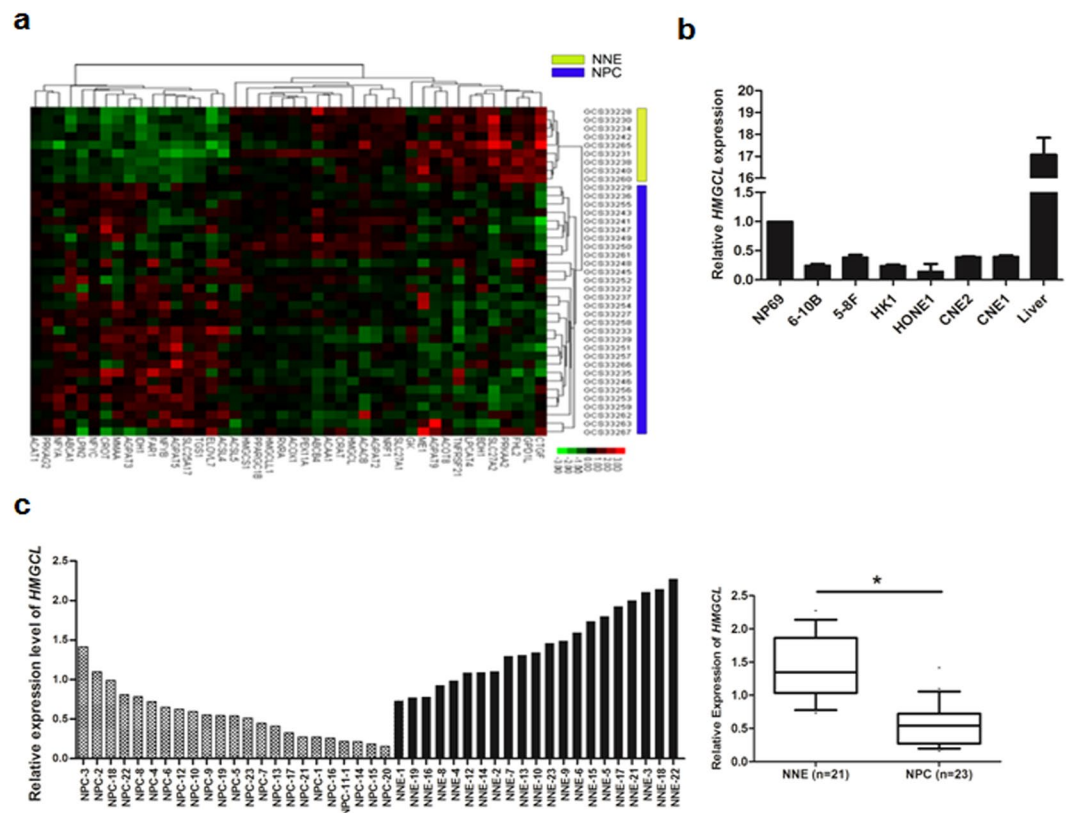


Figure 1. Transcription of *HMGCL* is downregulated in nasopharyngeal carcinoma (NPC). (a) A heat map showing 41 differentially expressed genes involved in lipid metabolism in NPC ($n = 30$) compared with normal nasopharyngeal epithelium (NNE, $n = 9$) based on cDNA microarray data (GSE 12452). (b) Real-time RT-PCR analysis of the mRNA level of *HMGCL* in 6 NPC cell lines and a non-cancerous nasopharyngeal epithelial cell line NP69. Human liver tissue was used as a positive control. (c) Real-time RT-PCR analysis of the mRNA level of *HMGCL* in NPC primary tumors ($n = 23$) and NNE tissue ($n = 21$). Boxes indicate 25 to 75 percentile, horizontal line indicates the mean, and bars indicate 10 and 90 percentiles. ($*p < 0.05$).

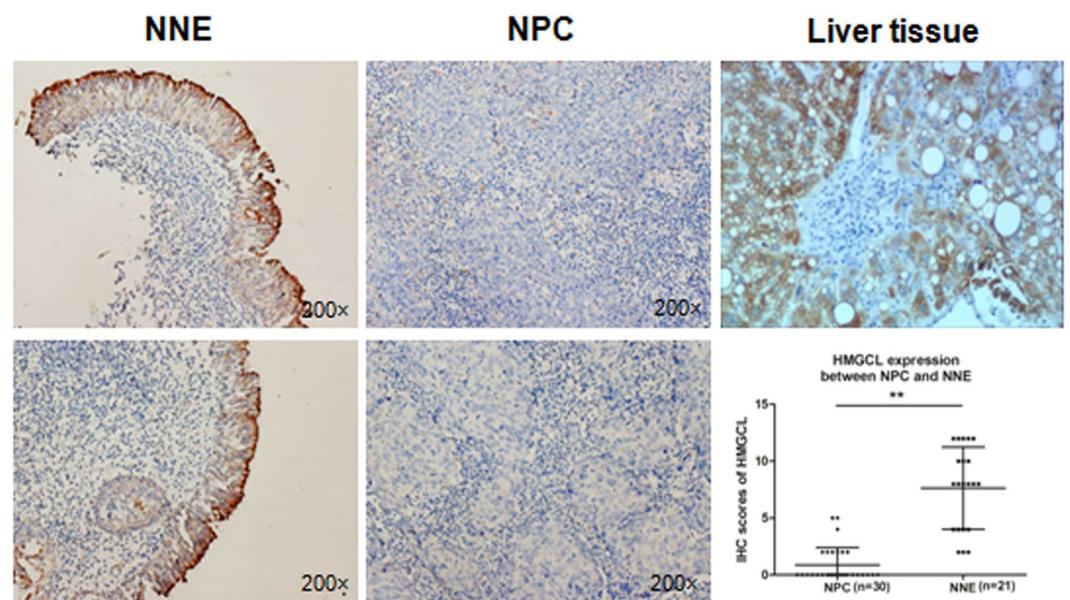


Figure 2. The expression of *HMGCL* is downregulated in NPC. Immunohistochemical staining of *HMGCL* in NPC ($n = 30$) and NNE tissue ($n = 21$). Representative images are immunostaining results for 2 NNE and 2 NPC samples (magnification $\times 200$). The scored *HMGCL* expression is shown in the scatter plot. Human liver tissue was used as a positive control. ($**p < 0.01$).

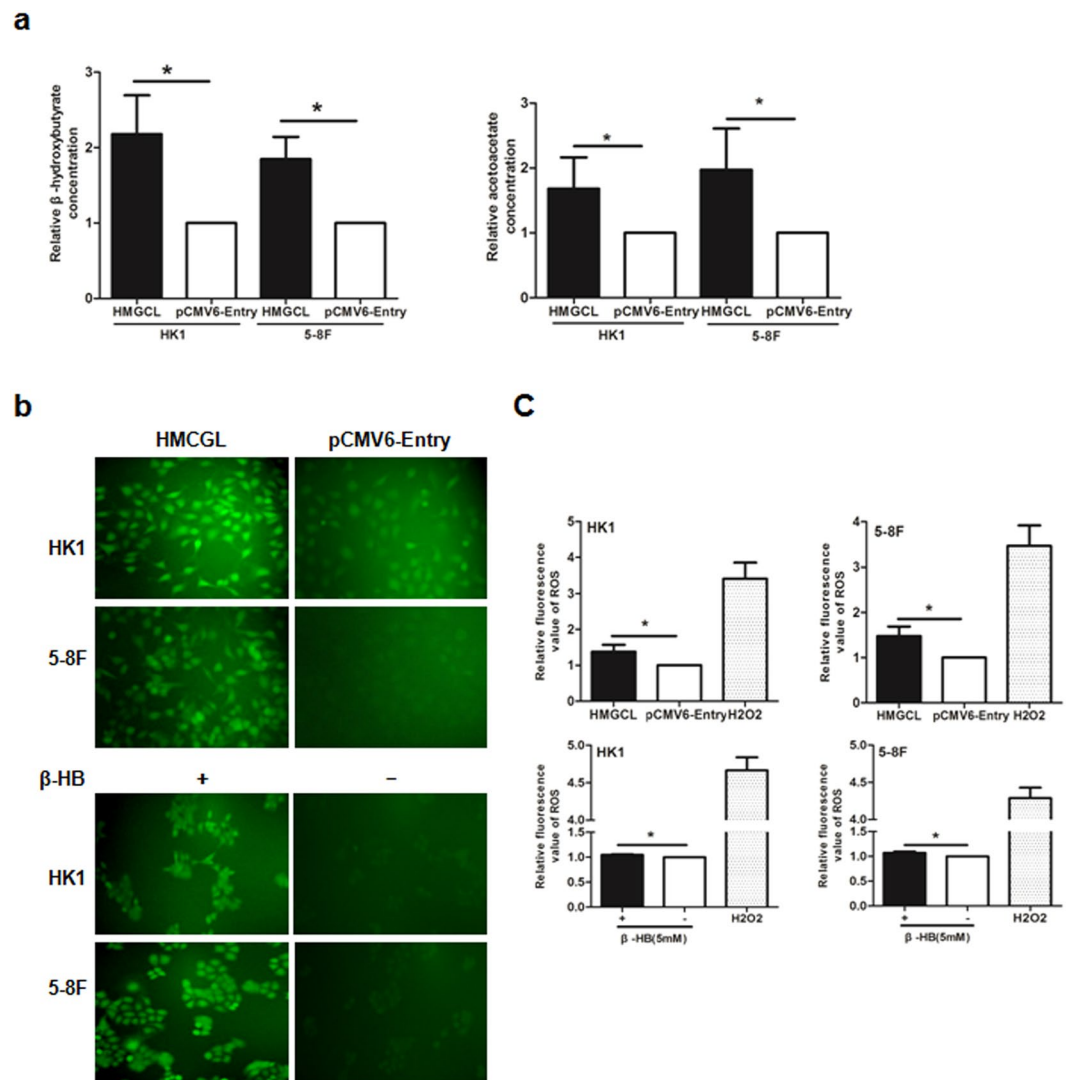


Figure 3. HMGCL elevates intracellular level of β -hydroxybutyrate (β -HB) and acetoacetate (AcAc) to increase reactive oxygen species (ROS) generation in NPC cells. **(a)** Relative concentration of intracellular β -HB and AcAc in HMGCL-HK1 and pCMV6-Entry-HK1 cells. Data are mean \pm SD ($n = 3$). **(b)** Detection of ROS by DCFH-DA probe with green fluorescent signals in HMGCL-HK1/5-8F and pCMV6-Entry-HK1/5-8F cells. Parental HK1 and 5-8F cells were treated with 5 mM β -HB for 24 h before ROS detection (magnification $\times 200$). **(c)** The fluorescent signals were also detected by a plate reader. Cells treated with H₂O₂ (50 μ g/ml) for 30 min was used as a positive control of ROS detection. Data are mean \pm SD ($n = 3$). (* $p < 0.05$).

HMGCL grew significantly slower than pCMV6-Entry-HK1/5-8F control cells (Fig. 4b, $P < 0.05$). Fewer colonies were observed in HMGCL-HK1/5-8F than control cells (Fig. 4c).

To determine whether the effect of HMGCL expression on tumor suppression could be reproduced *in vivo*, we subcutaneously injected HMGCL-5-8F and pCMV6-Entry-5-8F cells in opposite flanks of nude mice. Tumor volume was smaller with inoculation of HMGCL-5-8F than pCMV6-Entry-5-8F cells (Fig. 5a,b). IHC staining of the tumors confirmed the increased expression of HMGCL in tumors from HMGCL-5-8F injection (Fig. 5c). Taken together, exogenous expression of HMGCL may inhibit the growth of NPC cells both *in vitro* and *in vivo*.

Exogenous expression of HMGCL inhibits NPC cell migration and invasion by reversing the epithelial–mesenchymal transition (EMT). A metabolic shift, including glycolysis and ROS generation, contributes to NPC metastasis^{38,39}. To investigate the role of HMGCL in the metastatic potential of NPC cells, we used 2D and 3D model systems to determine the capacity for migration and invasion, respectively. In scratch assay, the gap closure was slower for HMGCL-HK1/5-8F than pCMV6-Entry-HK1/5-8F cells, indicating that HMGCL expression retarded the migration of NPC cells (Fig. 6a). Transwell assay also confirmed that overexpression of HMGCL markedly inhibited the invasive capacity of HK1 and 5-8F cells (Fig. 6b).

To reveal the underlying mechanism of HMGCL, we evaluated its effect on key EMT-associated proteins. The expression of E-cadherin was upregulated in HMGCL-HK1/5-8F cells and that of β -catenin and vimentin was

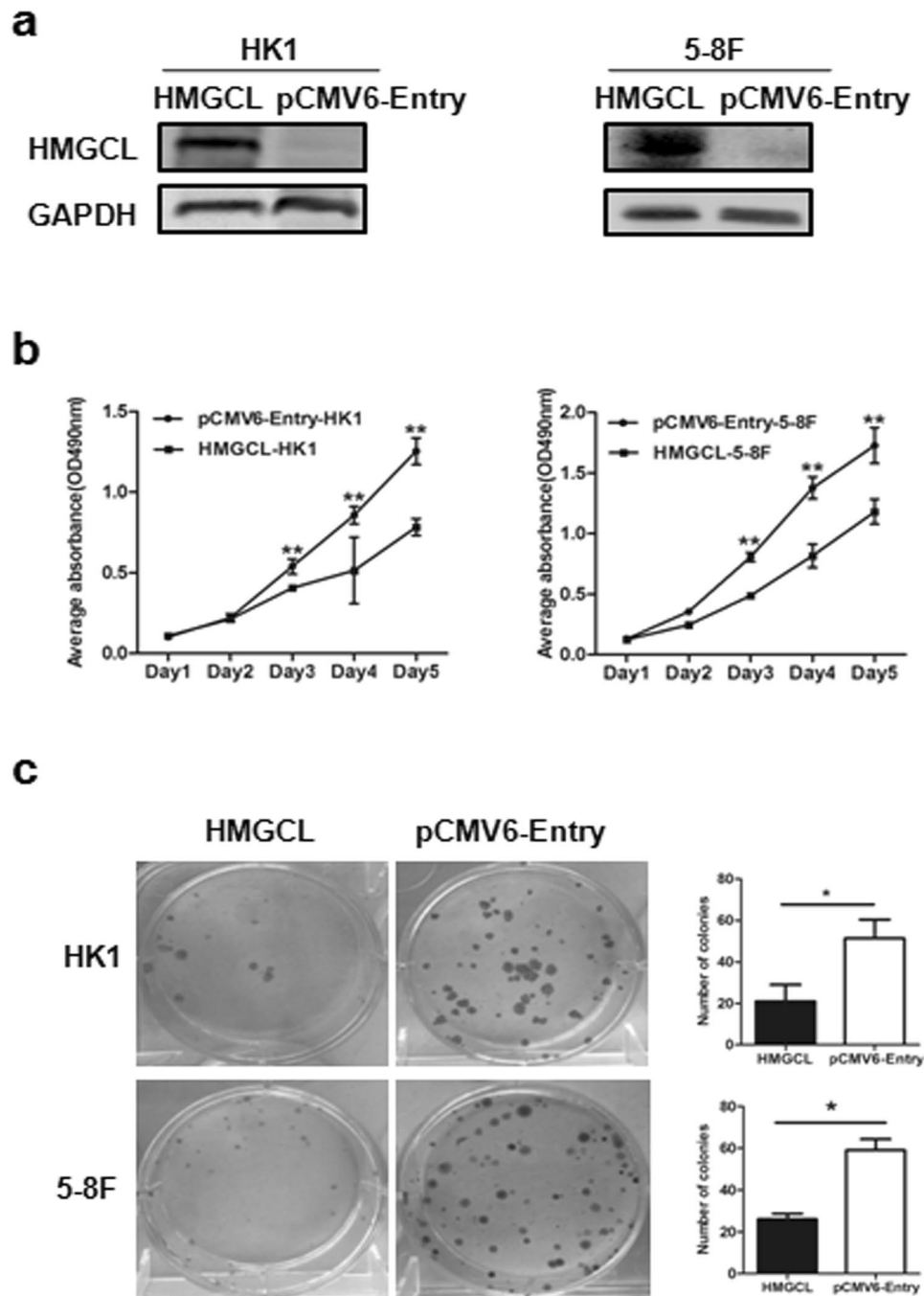


Figure 4. Exogenous expression of *HMGCL* suppresses proliferation and colony formation of NPC cells *in vitro*. (a) The expression of *HMGCL* in HK1 and 5-8 F cell lines was confirmed by Western blot. (b) MTT assay of growth curves for HK1 and 5-8 F cells (OD = 490 nm). (c) Colony formation assay of HK1 and 5-8 F cells for 12 days. Data are mean \pm SD (n = 3) (* p < 0.05; ** p < 0.01).

decreased (Fig. 6c). Accordingly, decreasing *HMGCL* expression in NPC cell lines may be involved in the EMT process and promote migration and invasion. Overexpression of *HMGCL* may reverse the EMT process, thereby inhibiting the metastasis potential of NPC cells.

ROS inhibitor promotes NPC cell growth and migration *in vitro*. To verify whether the inhibitory effect of *HMGCL* on NPC cells depends on ROS generation, we used the ROS inhibitor N-acetyl cysteine (NAC) to reduce the level of ROS in *HMGCL*-HK1/5-8 F cells. NAC treatment increased the proliferation of *HMGCL*-HK1/5-8 F cells (Fig. 7a) and reducing the ROS level in *HMGCL*-HK1/5-8 F cells accelerated their migratory capacity (Fig. 7b). The invasion of *HMGCL*-5-8F was enhanced by NAC (Fig. 7c). The inhibitory effect

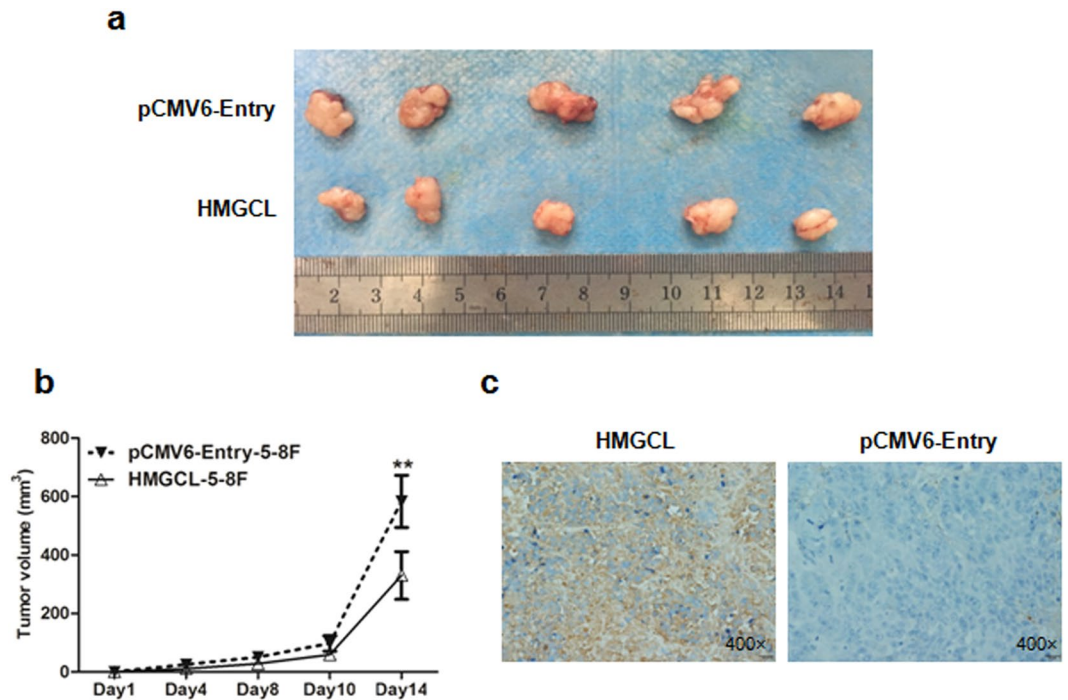


Figure 5. HMGCL suppresses tumorigenicity of NPC cells *in vivo*. (a) Xenografts from HMGCL-5-8F and pCMV6-Entry-5-8F cell injection were removed at day 14 after inoculation in nude mice. (b) Volume of the tumors was measured every 2 days after inoculation. (c) Immunohistochemical staining of HMGCL in removed tumors (magnification $\times 200$). ($*p < 0.05$).

of HMGCL on the growth and metastasis of NPC cells was reversed by treatment with the ROS inhibitor by inducing EMT (Fig. S1a), which suggests that ROS is a key mediator of HMGCL activity.

Extracellular β -HB inhibits NPC cell proliferation and migration depends on increasing ROS levels. Both intracellular and extracellular β -HB could stimulate ROS generation in NPC cells (Fig. 3b). Hence, we further evaluated the effect of extracellular β -HB on growth and motility of NPC cells. Growth and motility of HK1 cells were dose-dependently suppressed with β -HB treatment (Fig. 8a–c). Consistent with previous results, that β -HB treatment attenuates the migration of 5-8 F cells by reversing the EMT (Fig. S1b). However, AcAc did not play significant role as β -HB (Fig. S2). Furthermore, the combined treatment of β -HB and NAC increased the migration of HK1 cells (Fig. 8d). Therefore, the inhibitory effect of extracellular β -HB on NPC cells was similar to that of intracellular β -HB, relying on ROS generation.

Discussion

Many human cancers share metabolic alterations. In general, tumor cells metabolize glucose, lactate, pyruvate, hydroxybutyrate, acetate, glutamine, and FAs at much higher rates than do their non-tumor equivalents, which maximizes meeting the fundamental needs of proliferating cells²⁴. Targeting metabolic alteration has become a new avenue of therapeutic intervention in tumors.

By using an “*in silico*” approach, we analyzed the differential global transcription of genes involved in metabolic pathways in NPC compared to NNE tissue. HMGCL, a key enzyme in ketogenesis, was downregulated in NPC tissue. Both HMGCL transcription and protein expression was decreased in NPC cell lines and primary tumors. Besides of NPC, we also analyzed the RNA-sequencing database from the cancer genome atlas (TCGA) and found *HMGCL* transcription downregulated in several kinds of cancer, including head and neck, kidney and colon cancers (data not shown). Another ketogenic enzyme, HMGCS2, was found downregulated in colon cancer and associated with de-differentiation of colonic epithelium⁴⁰. These further suggest that altered ketogenesis may be a common feature in tumor tissue.

Intracellular long chain FAs undergo metabolism via two major pathways: esterification to build up FA esters (triglycerides, phospholipids) or oxidation to CO₂ and ketone bodies. In lung cancer, the mutation of *KRAS* promotes β -oxidation of FAs and the conversion of FAs into the acyl-CoA of FAs, which serve as substrates for lipid synthesis⁴¹. We previously found greater accumulation of LDs in NPC cells than NNE cells, which suggests elevated esterification of FAs in NPC²¹. In addition to downregulating HMGCL, this metabolic pathway might contribute to the reduced ketogenesis in NPC. Conversely, lack of induction of the ketogenesis enzyme HMGCS2 might contribute to impaired FA β -oxidation⁴².

In investigating the functional consequences of HMGCL downregulation in NPC, we detected an increased level of intracellular β -HB, a downstream product of HMGCL, in NPC cells stably transfected with HMGCL. Ketone-body metabolism may be critical for tumor progression and metastasis in NPC.

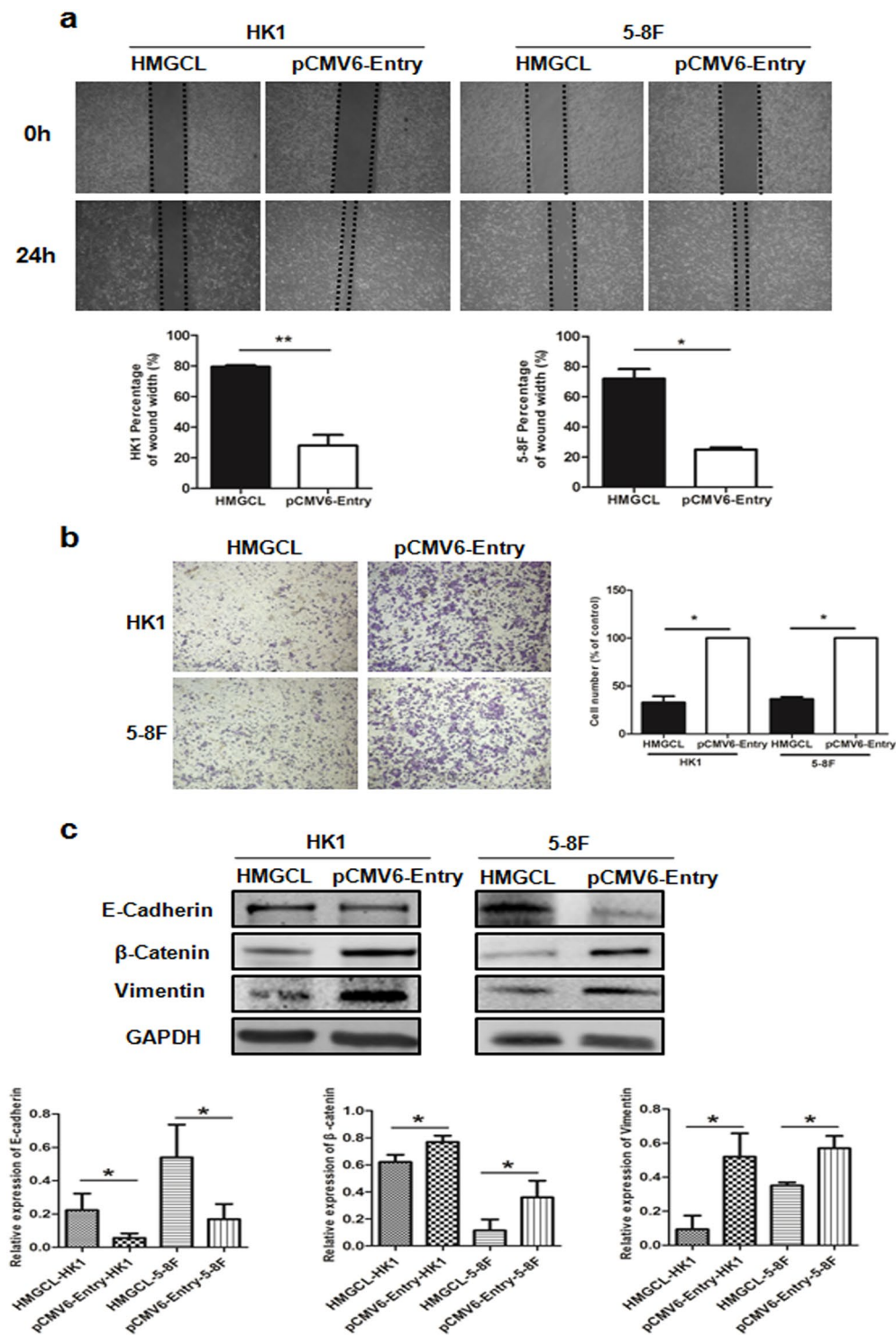


Figure 6. HMGCL inhibits NPC cell migration and invasion by reversing the epithelial–mesenchymal transition (EMT). **(a)** Wound healing assays of HMGCL-HK1/5-8 F and pCMV6-Entry-HK1/5-8 F cell lines. The gap was photographed and measured at 0 and 24 h. The percentage of wound width for each sample was calculated as $[\text{width } (\mu\text{m}) \text{ at } 24\text{h}] / [\text{width } (\mu\text{m}) \text{ at } 0\text{h}] \times 100\%$. **(b)** Transwell assay of invasive capacity of HMGCL-HK1/5-8 F and pCMV6-Entry-HK1/5-8 F cells. The blue dots represent the invading cells stained with crystal violet. The number of invading cells were counted and shown in the bar graph. **(c)** Western blot analysis of the expression of three key molecules involved in EMT, E-cadherin, β-catenin and Vimentin. GAPDH was an internal control. Data are mean \pm SD ($n = 3$). (* $p < 0.05$; ** $p < 0.01$).

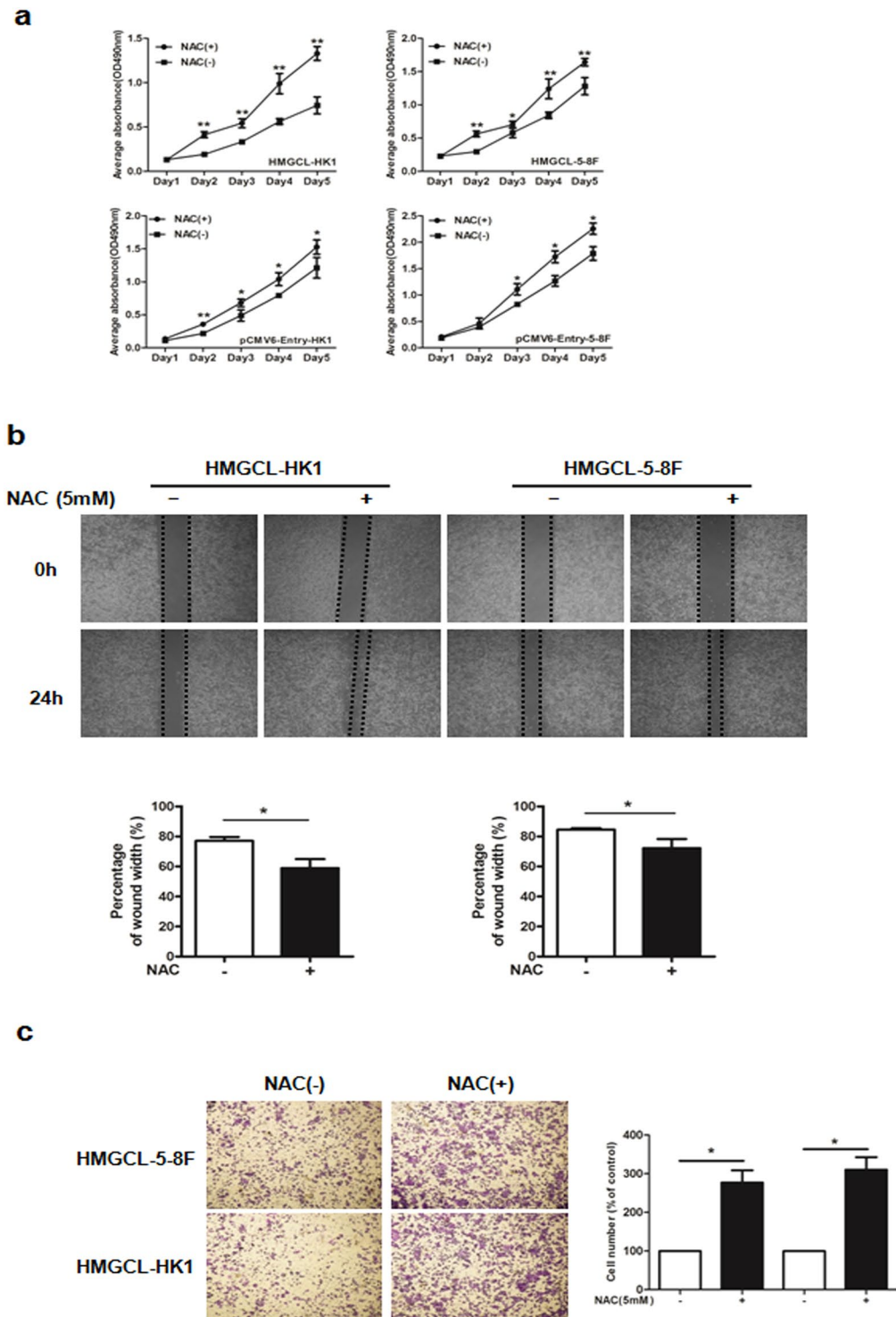


Figure 7. ROS inhibitor N-acetyl cysteine (NAC) accelerates NPC cell growth and migration *in vitro*. (a) The effect of NAC (5 mM) on proliferation of HMGCL-HK1/5-8 F and pCMV6-HK1/5-8 F cell lines measured by MTT assay. The effect of NAC (5 mM) on migratory (b) and invasive capacity (c) of HMGCL-HK1/5-8 F cells assessed by wound healing assay and transwell assay, respectively. Data are mean \pm SD (n = 3) (* p < 0.05; ** p < 0.01).

Ketogenic diet, as a novel approach in the treatment of cancer, has been discussed for a long time, but the clinical data are still limited⁴³. It has been shown that anti-tumor immunity is suppressed by inflammatory factor IL-6 by decreasing ketogenesis⁴⁴. In the contrary, a therapeutic ketogenic diet can enhance tumor-reactive immune responses⁴⁵. Ketogenic diet is suggested to have anti-cancer effect *in vitro* and *in vivo*^{31,46}, and could be applied for

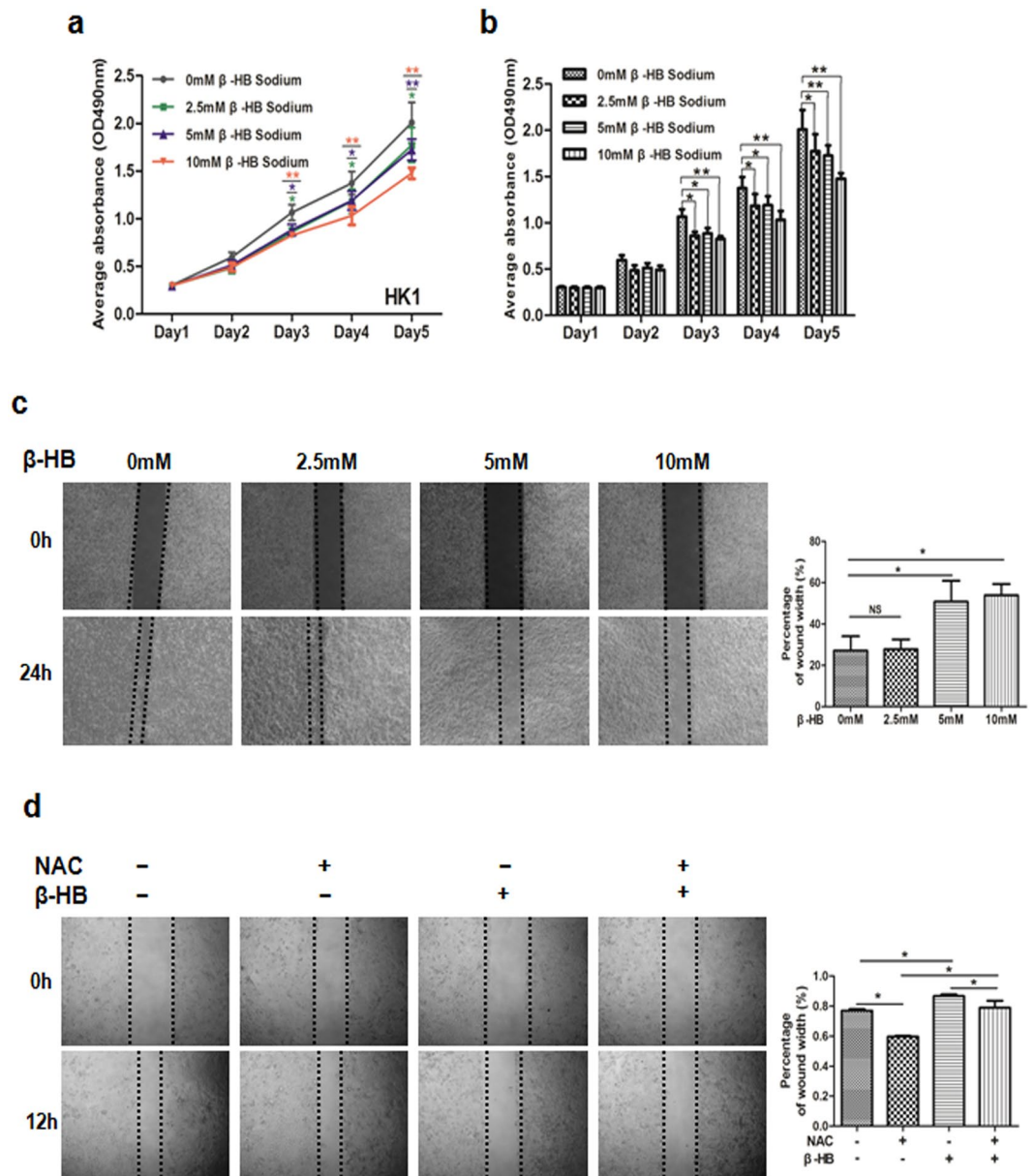


Figure 8. β -HB treatment inhibits NPC cell proliferation and migration. (a,b) MTT assay was performed to measure the proliferation of HK1 cells after β -HB treatment at 0 mM, 2.5 mM, 5 mM and 10 mM. (c) Motility of HK1 cells with various concentrations of β -HB. (d) Motility in HK1 cells with 5 mM NAC and 5 mM β -HB, alone or combined. Data are mean \pm SD (n = 3) (* p < 0.05; ** p < 0.01).

management of brain tumors in both preclinical and clinical settings⁴⁷. Hence, ketogenesis may be an undesirable metabolic characteristic of NPC cells and a target for NPC therapy.

We also found that β -HB treatment of NPC cells significantly decreased their viability, motility and proliferation and that this decrease could be reversed by the ROS antioxidant NAC. Thus, ROS is a major downstream mediator of the effects of intracellular ketone bodies, and the inhibition of proliferation caused by ketone bodies depends on ROS in NPC. In NPC tumors, every cell carries the EBV genome in a latent state. A low level of ROS might be essential for maintaining EBV infection. More than 120 genes are encoded by EBV, but only a few are expressed in NPC latent infection. This situation reduces the immunogenicity of the latently EBV-infected cells, thereby allowing them to evade immune attack. A recent study reported that increased ROS production could trigger the reactivation of EBV from latency in NPC cells⁴⁸. We also showed that knocking down a reductase, GLRX3, impaired the proliferation and metastasis of NPC cells by elevating the level of ROS³⁹. Hence, inhibition of ketogenesis by downregulating HMGCL may be one of the mechanisms involved in modulating EBV latent infection in NPC cells, thus contributing to tumorigenesis and progression by reducing the immunogenicity of NPC cells. This association of EBV latency and HMGCL expression in NPC needs further investigation.

Epigenetic mechanisms such as DNA methylation, histone modifications and microRNAs, which are altered in the EBV genome and in host cells, may underlie the initiation and progression of NPC⁴⁹. Dysregulated expression of histone deacetylases (HDACs) results in aberrant gene expression, thereby altering cellular functions, including malignant transformation⁵⁰. HDACs are also involved in maintaining the EBV latent cycle. HDAC inhibitors (HDACi) are potent inducers of EBV reactivation, which is critical for expression of lytic proteins, thereby providing novel targets for therapy as well as mediating the enhanced killing of cancer cells when used alone or with additional anti-cancer agents in EBV-associated malignancies^{51,52}. β -HB belongs to the endogenous inhibitors of HDACs. In addition, a lower level of β -HB impairs the differentiation of intestinal cells⁵³, which suggests an important role of ketone bodies in the development of epithelium. Therefore, elevating the level of β -HB by targeting a ketogenic gene might be a promising approach for NPC.

In summary, HMGCL was downregulated in NPC cells and tumor tissues. Overexpression of HMGCL in NPC cells increased the levels of ketone bodies and ROS, thereby inhibiting cell proliferation, suppressing EMT and reducing NPC cell invasion and migration. Our findings reveal a novel mechanism of NPC tumorigenesis that metabolism of ketone bodies may affect NPC cells by disrupting the redox balance of the intracellular environment. Thus, manipulating ketone-body metabolism might be a new area for drug discovery and dietary interventions for prevention and treatment of NPC.

Materials and Methods

Ethics statement. Ethical permission for this study was granted by the Research Ethics Committee of the First Affiliated Hospital of Guangxi Medical University, China (documents no.2016-KY-050). Written informed consent was obtained from all patients and healthy participants. All methods were performed in accordance with the relevant guidelines and regulations.

Study samples. NPC cell lines CNE1, CNE2, HONE1, HK1, 5-8 F and 6-10B were maintained in DMEM medium (Invitrogen, Carlsbad, CA, USA) supplemented with 10% fetal bovine serum (FBS; Invitrogen) in an atmosphere with 5% CO₂ at 37 °C^{54–57}. The nonmalignant nasopharyngeal epithelial cell line NP69 was grown in defined keratinocyte serum-free medium (Invitrogen)⁵⁸.

In total, 53 NPC primary tumor biopsies were collected from newly diagnosed and untreated NPC patients at the Department of Otolaryngology-Head and Neck Surgery, First Affiliated Hospital of Guangxi Medical University (Nanning, China). A total of 42 normal nasopharyngeal epithelium (NNE) tissue samples with chronic inflammation were included as controls. Overall, 23 NPC and 21 NNE samples were used for RNA extraction, and 30 NPC biopsies and 21 NNE samples were formalin-fixed and paraffin-embedded.

Antibodies, plasmids and reagents. Primary antibodies were for HMGCL (HPA004727; Sigma-Aldrich, St. Louis, MO, USA); β -catenin (sc-376841; Santa Cruz Biotechnology, Santa Cruz, CA, USA); and E-cadherin (#3195 P), Vimentin (#5741 P) and GAPDH (#5174 P; all Cell Signaling, Beverly, MA, USA). The secondary antibody 680RD goat anti-mouse and IRDye[®]800CW goat anti-rabbit antibody were from LI-COR Biosciences (Lincoln, NE, USA).

The full-length coding sequence for *HMGCL* subcloned into the pCMV6-Entry vector was from Origene (Rockville, MD, USA). Two NPC cell lines (HK1 and 5-8 F) were transfected with the pCMV6-Entry-*HMGCL* plasmid and empty-vector pCMV6-Entry, respectively, by using X-tremeGENE transfection reagents (#06366236001, Roche, Mannheim, Germany). Stable clones were obtained by selection in 400 μ g/ml G418 (#G8160, Solarbio, Beijing, China) for 2 weeks and maintained in medium with 250 μ g/ml G418. The ROS inhibitor N-acetyl-L-cysteine (NAC, #A7250) was from Sigma-Aldrich.

Quantitative Real-time PCR (qRT-PCR). Total RNA was extracted from cells and tissues by using TRIzol reagent (Invitrogen, Carlsbad, CA, USA) and cDNA synthesis involved use of the Prime Script RT reagent kit (Invitrogen, Carlsbad, CA, USA). The expression of *HMGCL* mRNA was determined by using Fast start universal green master mix in the ABI 7500 Real Time PCR system (Applied Biosystems, USA). Glyceraldehyde-3-phosphate dehydrogenase (GAPDH) was an internal control. The primer sequences were for *HMGCL*-F: 5'-ACCACCAGCTTTGTGTCTCC-3', *HMGCL*-R: 5'-GAGGCAGCTCCAAAGATGAC-3'; and *GAPDH*-F: 5'-GCACCGTCAAGGCTGAGAAC-3', *GAPDH*-R: 5'-TGGTGAAGACGCCAGTGA-3'.

Immunohistochemical staining. Tissues were cut into 3- μ m-thick sections and incubated for 1 h with 3% hydrogen peroxide to eliminate endogenous peroxidase activity after deparaffinization and rehydration. After antigen retrieval, sections were incubated with HMGCL antibody at 4 °C overnight, then secondary antibody for 1 h at room temperature. Subsequently, 3,3'-diaminobenzidine (DAB) reagent (ZLI-9018, ZSGB-BIO, Beijing) was used for peroxidase reaction and hematoxylin was used for counterstaining. Images were acquired under a microscope (Olympus C-5050, Japan). The immunohistochemistry results were independently evaluated by two pathologists who were blinded to sample status. The intensity of HMGCL staining was scored and graded as described⁵⁹.

β -hydroxybutyrate (β -HB) detection assay. Stably transfected cell lines pCMV6-Entry-HK1 and *HMGCL*-HK1 were grown in 100-mm dishes in serum-free DMEM medium for 48 h. Then cells were lysed with RIPA buffer (Beyotime, Jiangsu, China). Intracellular β -HB level was determined by using a β -HB colorimetric assay kit (#700190, Cayman Chemical, Ann Arbor, MI, USA). The concentration of β -HB was normalized to that of protein in the lysate.

ROS detection. Intracellular ROS was detected by use of a kit (S0033, Beyotime, Jiangsu, China). Briefly, adherent cells were incubated with DCFH-DA probe in serum-free DMEM medium at 37 °C for 30 min, then

washed with PBS three times and visualized under a fluorescent microscope or detected by a fluorescent reader (Biotek synergy HTX, USA).

Cell proliferation assay. Cells (2×10^3 cells per well) were seeded into 96-well plates and allowed to grow for 5 days to determine a growth curve. Cell density was examined every 24 h by use of 3-(4,5-dimethylthiazol-2-yl)-2,5-diphenyl tetrazolium bromide (MTT) assay (M1025, Solarbio, Beijing), in a plate reader with absorbance at OD490 nm (iMark, Bio-Rad, Hercules, CA, USA). Each experiment was performed in quintuplicate.

Colony formation assay. Cells (100 per well) were seeded in 6-well plates. The medium was changed every 3 days. After 14 days, Giemsa-stained colonies were photographed and counted by use of Quantity One v4.4.0 (Bio-Rad, USA). The experiment was performed in triplicate.

In vivo tumorigenicity assay. Five 4-week-old male BALB/c-nu nude mice (Experimental Animal Center of Guangxi Medical University, China) were injected with 1.0×10^6 pCMV6-Entry-5-8F cells in the right flank, and an equal amount of HMCGL-5-8F cells was injected into the left flank as a control. The tumor volume was assessed by 2D measurements every 2 days. Tumor volume was calculated as volume (mm^3) = length \times width² \times 0.5. Two weeks after inoculation, all mice were killed and tumors were removed. The animal study was approved by the Animal Ethical Committee of First Affiliated Hospital of Guangxi Medical University. All the methods were carried out in accordance with the approved guidelines.

Wound healing assay. Cells (5×10^5 per well) were seeded into 6-well plates and allowed to adhere overnight with DMEM medium without FBS. Monolayer cells were scratched by using a sterile 200- μ l pipette tip. The width of scratch was measured at 3 time points (0, 12 and 24 h) by light microscopy (CKX41, Olympus, Japan). The experiment was performed in triplicate.

Transwell assay. Cells (2.5×10^4 per well) resuspended in serum-free DMEM medium were seeded in the upper chamber of 24-well Bio-Coat Invasion Chambers (BD, Bedford, MA, USA) coated with Matrigel. The lower chamber was filled with DMEM medium with 10% FBS. Non-invading cells were removed by using a cotton-tipped swab at 48 h. Migratory and invasive cells on the lower membrane surface were fixed with 1% paraformaldehyde, stained with 0.5% crystal violet and photographed.

Western blot analysis. Proteins were separated by SDS-PAGE gel and transferred to nitrocellulose membranes (HATF00010, Millipore, Ireland), which were blocked with skim milk for 2 h at room temperature, then incubated with primary antibodies overnight at 4 °C followed by secondary antibody for 1 h at room temperature. The blotted proteins were detected and quantified by using a CCD camera in a ChemiDoc XRS instrument (Bio-Rad, USA) with Image Lab software.

Statistical analysis. All data were analyzed by using SPSS v16.0 (SPSS Inc., Chicago, IL, USA). Data are expressed as mean \pm SD and were analyzed by Pearson's chi-square test and Fisher's exact test. Statistical significance was considered at $p < 0.05$.

Data availability. The microarray datasets analyzed during the current study are available in the PubMed repository: <https://www.ncbi.nlm.nih.gov/sites/GDSbrowser?acc=GDS3341>.

References

- Chang, E. T. & Adami, H. O. The enigmatic epidemiology of nasopharyngeal carcinoma. *Cancer Epidemiol Biomarkers Prev* **15**, 1765–1777, doi:10.1158/1055-9965.EPI-06-0353 (2006).
- Tao, Q. & Chan, A. T. Nasopharyngeal carcinoma: molecular pathogenesis and therapeutic developments. *Expert Rev Mol Med* **9**, 1–24, doi:10.1017/S1462399407000312 (2007).
- Yu, K. H. *et al.* Survival outcome of patients with nasopharyngeal carcinoma with first local failure: a study by the Hong Kong Nasopharyngeal Carcinoma Study Group. *Head Neck* **27**, 397–405, doi:10.1002/hed.20161 (2005).
- Hanahan, D. & Weinberg, R. A. Hallmarks of cancer: the next generation. *Cell* **144**, 646–674, doi:10.1016/j.cell.2011.02.013 (2011).
- Lee, N. & Kim, D. Cancer Metabolism: Fueling More than Just Growth. *Mol Cells*, doi:10.14348/molcells.2016.0310 (2016).
- Tarrado-Castellarnau, M., Azañón, P. & Cascante, M. Oncogenic regulation of tumor metabolic reprogramming. *Oncotarget* **7**, 62726–62753, doi:10.18632/oncotarget.10911 (2016).
- Chang, C. H. *et al.* Metabolic Competition in the Tumor Microenvironment Is a Driver of Cancer Progression. *Cell* **162**, 1229–1241, doi:10.1016/j.cell.2015.08.016 (2015).
- Bayley, J. P. & Devilee, P. The Warburg effect in 2012. *Curr Opin Oncol* **24**, 62–67, doi:10.1097/CCO.0b013e32834deb9e (2012).
- Lo, A. K. *et al.* Activation of the FGFR1 signalling pathway by the Epstein-Barr virus-encoded LMP1 promotes aerobic glycolysis and transformation of human nasopharyngeal epithelial cells. *J Pathol* **237**, 238–248, doi:10.1002/path.4575 (2015).
- Jiang, Y. *et al.* Repression of Hox genes by LMP1 in nasopharyngeal carcinoma and modulation of glycolytic pathway genes by HoxC8. *Oncogene* **34**, 6079–6091, doi:10.1038/ncr.2015.53 (2015).
- Wong, E. Y. *et al.* TP53-induced glycolysis and apoptosis regulator promotes proliferation and invasiveness of nasopharyngeal carcinoma cells. *Oncol Lett* **9**, 569–574, doi:10.3892/ol.2014.2797 (2015).
- Zou, Z. W. *et al.* LncRNA ANRIL is up-regulated in nasopharyngeal carcinoma and promotes the cancer progression via increasing proliferation, reprogramming cell glucose metabolism and inducing side-population stem-like cancer cells. *Oncotarget* **7**, 61741–61754, doi:10.18632/oncotarget.11437 (2016).
- Li, H. *et al.* MiR-34b-3 and miR-449a inhibit malignant progression of nasopharyngeal carcinoma by targeting lactate dehydrogenase A. *Oncotarget* **7**, 54838–54851, doi:10.18632/oncotarget.10761 (2016).
- Parralés, A. & Iwakuma, T. p53 as a Regulator of Lipid Metabolism in Cancer. *Int J Mol Sci* **17**, doi:10.3390/ijms17122074 (2016).
- Pascual, G. *et al.* Targeting metastasis-initiating cells through the fatty acid receptor CD36. *Nature* **541**, 41–45, doi:10.1038/nature20791 (2017).
- Santos, C. R. & Schulze, A. Lipid metabolism in cancer. *FEBS J* **279**, 2610–2623, doi:10.1111/j.1742-4658.2012.08644.x (2012).
- Khan, A., Aljarbou, A. N., Aldebasi, Y. H., Faisal, S. M. & Khan, M. A. Resveratrol suppresses the proliferation of breast cancer cells by inhibiting fatty acid synthase signaling pathway. *Cancer Epidemiol* **38**, 765–772, doi:10.1016/j.canep.2014.09.006 (2014).

18. Tirinato, L. *et al.* Lipid droplets: a new player in colorectal cancer stem cells unveiled by spectroscopic imaging. *Stem Cells* **33**, 35–44, doi:10.1002/stem.1837 (2015).
19. Patel, A. V., Johansson, G., Colbert, M. C., Dasgupta, B. & Ratner, N. Fatty acid synthase is a metabolic oncogene targetable in malignant peripheral nerve sheath tumors. *Neuro Oncol* **17**, 1599–1608, doi:10.1093/neuonc/nov076 (2015).
20. Yasumoto, Y. *et al.* Inhibition of Fatty Acid Synthase Decreases Expression of Stemness Markers in Glioma Stem Cells. *PLoS One* **11**, e0147717, doi:10.1371/journal.pone.0147717 (2016).
21. Zhou, X. *et al.* Epigenetic downregulation of the ISG15-conjugating enzyme UbcH8 impairs lipolysis and correlates with poor prognosis in nasopharyngeal carcinoma. *Oncotarget* **6**, 41077–41091, doi:10.18632/oncotarget.6218 (2015).
22. Daker, M., Bhuvanendran, S., Ahmad, M., Takada, K. & Khoo, A. S. Deregulation of lipid metabolism pathway genes in nasopharyngeal carcinoma cells. *Mol Med Rep* **7**, 731–741, doi:10.3892/mmr.2012.1253 (2013).
23. Park, G. B. & Kim, D. Casticin inhibits epithelial-mesenchymal transition of EBV-infected human retina pigmented epithelial cells through the modulation of intracellular lipogenesis. *Graefes Arch Clin Exp Ophthalmol*, doi:10.1007/s00417-016-3551-3 (2016).
24. Martinez-Outschoorn, U. E., Peiris-Pages, M., Pestell, R. G., Sotgia, F. & Lisanti, M. P. Cancer metabolism: a therapeutic perspective. *Nat Rev Clin Oncol* **14**, 11–31, doi:10.1038/nrclinonc.2016.60 (2017).
25. Adjianto, J. *et al.* The retinal pigment epithelium utilizes fatty acids for ketogenesis. *J Biol Chem* **289**, 20570–20582, doi:10.1074/jbc.M114.565457 (2014).
26. Saraon, P. *et al.* Quantitative proteomics reveals that enzymes of the ketogenic pathway are associated with prostate cancer progression. *Mol Cell Proteomics* **12**, 1589–1601, doi:10.1074/mcp.M112.023887 (2013).
27. Kang, H. B. *et al.* Metabolic Rewiring by Oncogenic BRAF V600E Links Ketogenesis Pathway to BRAF-MEK1 Signaling. *Mol Cell* **59**, 345–358, doi:10.1016/j.molcel.2015.05.037 (2015).
28. Martinez-Outschoorn, U. E. *et al.* Ketone body utilization drives tumor growth and metastasis. *Cell Cycle* **11**, 3964–3971, doi:10.4161/cc.22137 (2012).
29. Magee, B. A., Potezny, N., Rofe, A. M. & Conyers, R. A. The inhibition of malignant cell growth by ketone bodies. *Aust J Exp Biol Med Sci* **57**, 529–539 (1979).
30. Shukla, S. K. *et al.* Metabolic reprogramming induced by ketone bodies diminishes pancreatic cancer cachexia. *Cancer Metab* **2**, 18, doi:10.1186/2049-3002-2-18 (2014).
31. Sawai, M., Yashiro, M., Nishiguchi, Y., Ohira, M. & Hirakawa, K. Growth-inhibitory effects of the ketone body, monoacetoacetin, on human gastric cancer cells with succinyl-CoA: 3-oxoacid CoA-transferase (SCOT) deficiency. *Anticancer Res* **24**, 2213–2217 (2004).
32. Du, X. *et al.* Acetoacetate induces hepatocytes apoptosis by the ROS-mediated MAPKs pathway in ketotic cows. *Journal of cellular physiology*, doi:10.1002/jcp.25773 (2017).
33. Berger, T., Saunders, M. E. & Mak, T. W. Beyond the Oncogene Revolution: Four New Ways to Combat Cancer. *Cold Spring Harbor symposia on quantitative biology*, doi:10.1101/sqb.2016.81.031161 (2017).
34. Fu, Z. *et al.* Crystal structure of human 3-hydroxy-3-methylglutaryl-CoA Lyase: insights into catalysis and the molecular basis for hydroxymethylglutaric aciduria. *J Biol Chem* **281**, 7526–7532, doi:10.1074/jbc.M506880200 (2006).
35. Martinez-Outschoorn, U. E. *et al.* Ketone bodies and two-compartment tumor metabolism: stromal ketone production fuels mitochondrial biogenesis in epithelial cancer cells. *Cell Cycle* **11**, 3956–3963, doi:10.4161/cc.22136 (2012).
36. Hu, H. *et al.* Genome-Wide Mapping of the Binding Sites and Structural Analysis of Kaposi's Sarcoma-Associated Herpesvirus Viral Interferon Regulatory Factor 2 Reveal that It Is a DNA-Binding Transcription Factor. *J Virol* **90**, 1158–1168, doi:10.1128/JVI.01392-15 (2015).
37. Kanikarla-Marie, P. & Jain, S. K. 1,25(OH)₂D₃ inhibits oxidative stress and monocyte adhesion by mediating the upregulation of GCLC and GSH in endothelial cells treated with acetoacetate (ketosis). *J Steroid Biochem Mol Biol* **159**, 94–101, doi:10.1016/j.jsbmb.2016.03.002 (2016).
38. Shen, Y. A., Wang, C. Y., Hsieh, Y. T., Chen, Y. J. & Wei, Y. H. Metabolic reprogramming orchestrates cancer stem cell properties in nasopharyngeal carcinoma. *Cell Cycle* **14**, 86–98, doi:10.4161/15384101.2014.974419 (2015).
39. He, F. *et al.* Glutaredoxin 3 promotes nasopharyngeal carcinoma growth and metastasis via EGFR/Akt pathway and independent of ROS. *Oncotarget* **7**, 37000–37012, doi:10.18632/oncotarget.9454 (2016).
40. Camarero, N. *et al.* Ketogenic HMGCS2 Is a c-Myc target gene expressed in differentiated cells of human colonic epithelium and down-regulated in colon cancer. *Mol Cancer Res* **4**, 645–653, doi:10.1158/1541-7786.MCR-05-0267 (2006).
41. Padanad, M. S. *et al.* Fatty Acid Oxidation Mediated by Acyl-CoA Synthetase Long Chain 3 Is Required for Mutant KRAS Lung Tumorigenesis. *Cell Rep* **16**, 1614–1628, doi:10.1016/j.celrep.2016.07.009 (2016).
42. Le May, C. *et al.* Reduced hepatic fatty acid oxidation in fasting PPARalpha null mice is due to impaired mitochondrial hydroxymethylglutaryl-CoA synthase gene expression. *FEBS Lett* **475**, 163–166 (2000).
43. Smyl, C. Ketogenic Diet and Cancer—a Perspective. Recent results in cancer research. *Fortschritte der Krebsforschung. Progres dans les recherches sur le cancer* **207**, 233–240, doi:10.1007/978-3-319-42118-6_11 (2016).
44. Flint, T. R. *et al.* Tumor-Induced IL-6 Reprograms Host Metabolism to Suppress Anti-tumor Immunity. *Cell Metab* **24**, 672–684, doi:10.1016/j.cmet.2016.10.010 (2016).
45. Lussier, D. M. *et al.* Enhanced immunity in a mouse model of malignant glioma is mediated by a therapeutic ketogenic diet. *BMC cancer* **16**, 310, doi:10.1186/s12885-016-2337-7 (2016).
46. Skinner, R., Trujillo, A., Ma, X. & Beierle, E. A. Ketone bodies inhibit the viability of human neuroblastoma cells. *J Pediatr Surg* **44**(discussion 216), 212–216, doi:10.1016/j.jpedsurg.2008.10.042 (2009).
47. Vidali, S. *et al.* Mitochondria: The ketogenic diet—A metabolism-based therapy. *Int J Biochem Cell Biol* **63**, 55–59, doi:10.1016/j.biocel.2015.01.022 (2015).
48. Huang, S. Y. *et al.* Reactive oxygen species mediate Epstein-Barr virus reactivation by N-methyl-N'-nitro-N-nitrosoguanidine. *PloS one* **8**, e84919, doi:10.1371/journal.pone.0084919 (2013).
49. Shyamasundar, S., Dheen, S. T. & Bay, B. H. Histone Modifications as Molecular Targets in Nasopharyngeal Cancer. *Curr Med Chem* **23**, 186–197 (2016).
50. Ropero, S. & Esteller, M. The role of histone deacetylases (HDACs) in human cancer. *Mol Oncol* **1**, 19–25, doi:10.1016/j.molonc.2007.01.001 (2007).
51. Hui, K. F. *et al.* Activation of lytic cycle of Epstein-Barr virus by suberoylanilide hydroxamic acid leads to apoptosis and tumor growth suppression of nasopharyngeal carcinoma. *Int J Cancer* **131**, 1930–1940, doi:10.1002/ijc.27439 (2012).
52. Hui, K. F., Lam, B. H., Ho, D. N., Tsao, S. W. & Chiang, A. K. Bortezomib and SAHA synergistically induce ROS-driven caspase-dependent apoptosis of nasopharyngeal carcinoma and block replication of Epstein-Barr virus. *Mol Cancer Ther* **12**, 747–758, doi:10.1158/1535-7163.MCT-12-0811 (2013).
53. Wang, Q. *et al.* Ketogenesis contributes to intestinal cell differentiation. *Cell Death Differ*, doi:10.1038/cdd.2016.142 (2016).
54. Glaser, R. *et al.* Two epithelial tumor cell lines (HNE-1 and HONE-1) latently infected with Epstein-Barr virus that were derived from nasopharyngeal carcinomas. *Proc Natl Acad Sci USA* **86**, 9524–9528 (1989).
55. Huang, D. P. *et al.* Establishment of a cell line (NPC/HK1) from a differentiated squamous carcinoma of the nasopharynx. *Int J Cancer* **26**, 127–132 (1980).
56. Fang, W. Y. *et al.* Reexploring the possible roles of some genes associated with nasopharyngeal carcinoma using microarray-based detection. *Acta Biochim Biophys Sin (Shanghai)* **37**, 541–546 (2005).

57. Sizhong, Z., Xiukung, G. & Yi, Z. Cytogenetic studies on an epithelial cell line derived from poorly differentiated nasopharyngeal carcinoma. *Int J Cancer* **31**, 587–590 (1983).
58. Tsao, S. W. *et al.* Establishment of two immortalized nasopharyngeal epithelial cell lines using SV40 large T and HPV16E6/E7 viral oncogenes. *Biochim Biophys Acta* **1590**, 150–158 (2002).
59. Wang, J. *et al.* Downregulation of stathmin 1 in human gallbladder carcinoma inhibits tumor growth *in vitro* and *in vivo*. *Sci Rep* **6**, 28833, doi:10.1038/srep28833 (2016).

Acknowledgements

We thank Dr. Liumila Matskova (Karolinska Institutet, Sweden) and Dr. Gösta Winberg (Ludwig Institute for Cancer Research, Sweden) for their useful comments. This study was supported by grants from the National Natural Science Foundation of China (81660458).

Author Contributions

Conception and design: X.Y.Z. and P.L.; investigation and data acquisition: W.Q.L. and L.T.Q., Z.P.L., Y.X.M.; analysis and interpretation of data: W.Q.L., J.Z.L., X.L.X., and B.L.; material support: X.X., and Z.Z.; writing, review, and/or revision of the manuscript: W.Q.L., Z.Z., G.W.H., X.Y.Z. and P.L.; study supervision: P.L., and X.Y.Z.; funding receiver: P.L.

Additional Information

Supplementary information accompanies this paper at doi:10.1038/s41598-017-11025-2

Competing Interests: The authors declare that they have no competing interests.

Publisher's note: Springer Nature remains neutral with regard to jurisdictional claims in published maps and institutional affiliations.



Open Access This article is licensed under a Creative Commons Attribution 4.0 International License, which permits use, sharing, adaptation, distribution and reproduction in any medium or format, as long as you give appropriate credit to the original author(s) and the source, provide a link to the Creative Commons license, and indicate if changes were made. The images or other third party material in this article are included in the article's Creative Commons license, unless indicated otherwise in a credit line to the material. If material is not included in the article's Creative Commons license and your intended use is not permitted by statutory regulation or exceeds the permitted use, you will need to obtain permission directly from the copyright holder. To view a copy of this license, visit <http://creativecommons.org/licenses/by/4.0/>.

© The Author(s) 2017